This article has been accepted for publication in a future issue of this journal, but has not been fully edited. Content may change prior to final publication. Citation information: DOI 10.1109/TNB.2016.2628047, IEEE Transactions on NanoBioscience

An End-to-end Model of Plant Pheromone Channel for Long Range Molecular Communication

Bige D. Unluturk, *Student Member, IEEE,* Ian F. Akyildiz, *Fellow, IEEE*

***Abstract*—A new track in molecular communication is using pheromones which can scale up the range of diffusion-based communication from μmeters to meters and enable new applications requiring long range. Pheromone communication is the emission of molecules in the air which trigger behavioral or physiological responses in receiving organisms. The objective of this paper is to introduce a new end-to-end model which incorporates pheromone behavior with communication theory for plants. The proposed model includes both the transmission and reception processes as well as the propagation channel. The transmission process is the emission of pheromones from the leaves of plants. The dispersion of pheromones by the flow of wind constitutes the propagation process. The reception process is the sensing of pheromones by the pheromone receptors of plants. The major difference of pheromone communication from other molecular communication techniques is the dispersion channel acting under the laws of turbulent diffusion. In this paper, the pheromone channel is modeled as a Gaussian puff, i.e., a cloud of pheromone released instantaneously from the source whose dispersion follows a Gaussian distribution. Numerical results on the performance of the overall end-to-end pheromone channel in terms of normalized gain and delay are provided.**

***Index Terms*—Molecular communication, nanonetworks, pheromone communication, pheromone channel, channel modeling**

I. Introduction

MOLECULAR communication (MC) is an emerging bio-inspired technology which aims to study biological communication mechanisms and mimic them to design artificial biocompatible communication networks. MC techniques are identified by the channel in which molecules propagate from the transmitter to the receiver device. These techniques include diffusion-based MC [1], flow-based MC [2], bacterial chemotaxis based MC [3], and molecular motor based MC [4]. The common vulnerability of all of these techniques is their limited range. The longest achievable range by these techniques reaches only millimeters with bacterial chemotaxis. Pheromone channel extends this range up to hundreds of meters.

Pheromones are used for alarming and potential mating within a species, and for attracting or repelling other species [5]. By exchanging different pheromone signals, the members of a species share information messages necessary for the survival and organization of the group. Furthermore, some pheromones common to more than one species constitute a way of communication in between species, which eventually serves to protect the balance of an ecosystem by allowing or preventing the encounter of predators and preys. Thus, pheromones establish a huge network of living organisms sensing the environment, communicating with each other, and regulating the course of life.

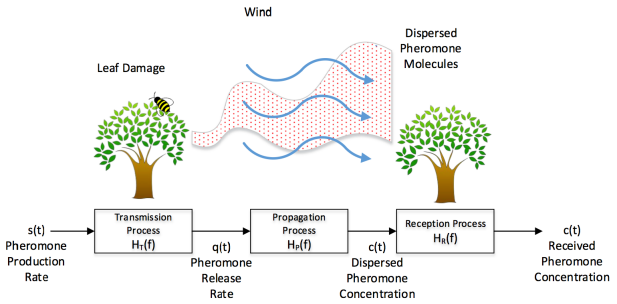

Fig. 1. End-to-end model for pheromone communication between plants.

The previously investigated MC techniques involve communication within the cell, among the cells and among nanoscale devices. However, pheromone communication takes place in all living organisms which may be either unicellular such as bacteria or multicellular such as animals and plants. Hence, pheromone communication can be used as an interface connecting MC at nanoscale to macro-world. By using long range MC techniques, nano-networks can access micro-scale devices which may further connect the system to internet, which integrates the classical communication and control methods to nanonetworks.

The application areas exploiting pheromone communication are agricultural applications including pest control by pheromone traps and mating disruption [17], and ecological applications for monitoring ecosystems and populations. Furthermore, due to fine sensing of pheromone receivers, the utilization of pheromone transmitter and receivers in industry will pave the way for new directions in air and water quality control.

Using pheromone channel for long range MC is first proposed in [14]. Then in [15], a very simple propagation model is described without taking into account the peculiarities of pheromone channels. Our objective is to lay down a solid channel model for one of the long range MC techniques, i.e., pheromone communication between plants, on top of which communication devices and model will be built.

Pheromone communication relies on the secretion of

This work was supported by the U.S. National Science Foundation (NSF) under the Grant CNS-1110947.

Bige D. Unluturk and I. F. Akyildiz are with the Broadband Wireless Networking Laboratory (BWN-Lab), School of Electrical and Computer Engineering, Georgia Institute of Technology, Atlanta, GA 30332 (e-mail: {bigedeniz, ian} @ece.gatech.edu). Phone: +1 404 894 6616, Fax: +1 404 894 7883.

This article has been accepted for publication in a future issue of this journal, but has not been fully edited. Content may change prior to final publication. Citation information: DOI 10.1109/TNB.2016.2628047, IEEE Transactions on NanoBioscience

pheromone molecules by the source organism into the air or water where molecules are propagated to the destination organism by the flow and the turbulent diffusion. Pheromone propagation is mostly studied in biology especially for insects. However, the focus of these studies are the biochemistry of the pheromone secretion and the impacts of pheromones on the recipients [5]. The studies on the propagation of pheromone molecules are very limited [6], [8], [11].

The unique feature of pheromone communication is the propagation based on both advection and turbulent diffusion [9]–[11]. The pheromone trail emitted by a plant leaf in air follows a Gaussian puff model whose shape depends on the characteristics of the wind and atmospheric stability [8]. Furthermore, the diffusion constants change according to the distance and the atmospheric parameters. This behavior can not be captured by the previous propagation models in the literature [12], [13] which use constant diffusion coefficients and investigate the effects of advection only in the flow direction neglecting the turbulent diffusion created by the advection on the other two dimensions. We will incorporate the communication theory with these studies in order to build a model for the pheromone communication mechanism and investigate the performance of this emerging communication technique.

In this study, we chose plants as pheromone transmitter and receiver which are naturally using pheromones to communicate with each other as shown in Fig. 1 [7]. However, modeling the transmission and reception of pheromones by plants is a challenging task due to the complex structure of plant leaves despite the high number of studies experimentally proving the pheromone communication between plants. Emission of pheromones can be studied in leaf, plant, canopy and landscape scales [32]. We adopted a leaf-level approach for the transmitter where we consider the release of pheromones from a single stimulated leaf. The pheromone signals in the air are received by leaves which uptake pheromones into their intercellular air space by stomata. When the pheromones diffuse into cells of leaf, they activate physiological responses in the plant which consists the detection of the pheromone signals.

In this paper, the basic three steps of pheromone communication, namely, transmission, propagation and reception, are considered, and an end-to-end model is provided. Each step is modeled analytically and its normalized gain and delay are investigated. It is found that the range of pheromone communication is very directional due to the wind compared to the uniform range of diffusion-based MC where the molecules travel in every direction.

The rest of the paper is organized as follows. In Section II, the transmission process of pheromone signals is studied. Then, in section III, the dispersion of the pheromone signals in the atmosphere is analyzed. The reception mechanism of pheromone signals arriving to the destination plant is studied in Section IV. Numerical results for normalized gain and delay of the pheromone communication system are presented in Section V for each step and the whole end-to-end model. Finally we conclude our study in Sec. VI and discuss open research problems.

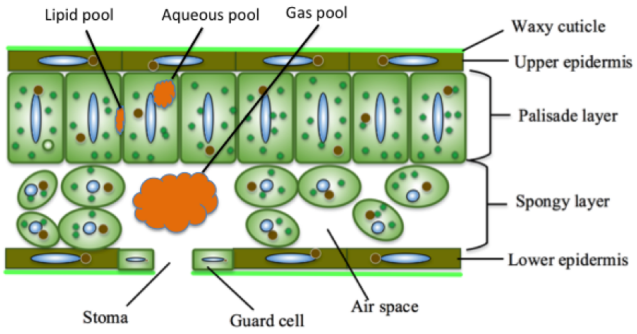

Fig. 2. Leaf cross-section showing stomata and intercellular air space [16]. The gas exchange between the intercellular air spaces and the environment is realized by the stomatas, i. e., pores under the leaf which are opened and closed by the guard cells. The upper and lower epidermis are the outer layer of cells covering the leaf which are often covered by a waxy cuticle creating a boundary between the internal cells and the environment. Example storage pools are shown only for one cell and one intercellular airspace.

II. The Transmission Process of Pheromone Signals

Pheromone communication is utilized by all organisms in nature. Hence there is a variety in pheromone molecules which are often bound to a specific message for a particular species. Furthermore, majority of the species can both produce and respond to thousands of different pheromone types at the same time. Thus, there is a pheromone diversity which allows different communication channels to co-exist without any interference. Also, a MC network composed of multiple nanomachines can exploit the pheromone diversity [15] by assigning a different pheromone type for each one-to-one link. Thus, an interference and contention-free nanonetwork can be built.

In this study, plants are chosen as the transmitters and receivers exchanging pheromone communication signals. The channel between two plants is assigned a single type of pheromone whose concentration is varied by the pheromone emission from a transmitter plant in response to an environmental change. For example, when a transmitter plant senses a change in its environment, it warns its conspecifics from the danger or repel the predators causing danger. For example, when plants in the field growing next to each other sense that they are too close to the neighbor plant, they secret a chemical which triggers the slowdown of the growth hormone production to prevent covering each others' leaves so that the two plants can both survive. Another example is the pheromone emission from the damaged leaf which summons the predators in case of a herbivore insect attack.

Plants emit pheromones from various locations on them such as glandular trichomes on their body [28] or leaves [29]. Usually, secretory cells produce the pheromone to be released prior to the excitation. Pheromone molecules are stored in vesicles either in the cell or in between the cell membrane and the cell wall. Then, upon the transfer of the message, the stored pheromone molecules are released to the medium. These secretory cells are placed in other cells with rigid walls to prevent the secreted pheromones from flowing back into the

This article has been accepted for publication in a future issue of this journal, but has not been fully edited. Content may change prior to final publication. Citation information: DOI 10.1109/TNB.2016.2628047, IEEE Transactions on NanoBioscience

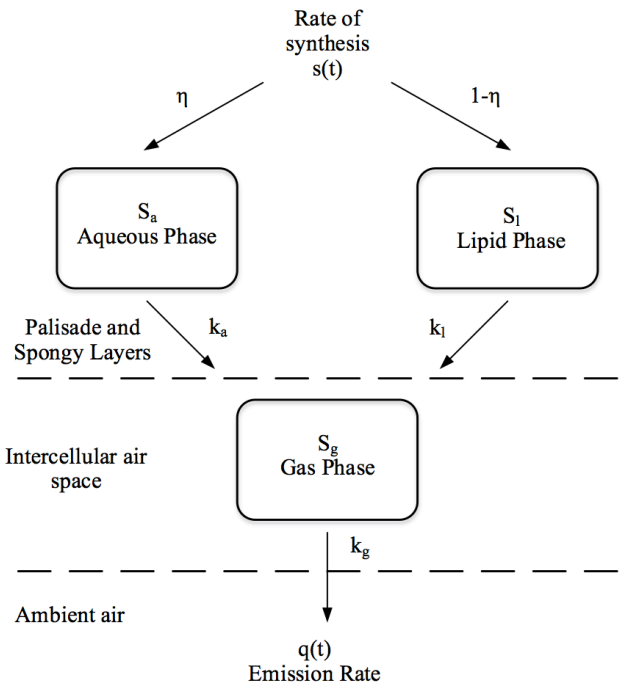

Fig. 3. Diffusion pathway of pheromones from source cells to air through the layers of the leaf [32].

plant [30].

There are two types of pheromone emission from the plant, namely, constitutive and stress-driven emissions. Every plant releases chemicals to its surroundings which are produced continuously, such as methanol emission during the expansion of a leaf, which is the constitutive emission independent of external triggering factors. However, when the plant undergoes a stress factor such as a herbivore attack or drought, it responds by instantaneously releasing chemicals stored in cells or in between cell walls as a defense mechanism, which is the stress-driven emission. In this study, we consider that pheromones are emitted from the leaves of a plant. The structure of a leaf which has many layers is shown in Fig. 2. The upper and lower epidermis are the outer layer of cells covering the leaf which are often covered by a waxy cuticle creating a boundary between the internal cells and the environment. The palisade layer consists of regularly arranged cells rich in chloroplasts whereas the spongy layer consists of cells which are not regularly stacked leaving large intercellular air spaces. The gas exchange between these intercellular air spaces and the environment is realized by the stomatas, i. e., pores under the leaf.

For both constitutive and stress-driven emissions, pheromones produced or released from the storage arrive to the intercellular air space. Then, pheromones are released to the air from stomata, i.e, pores under the leaves controlling gas exchange. However, the emission rate of pheromones is not the same as the production rate from which we deduce that there are temporary storage pools in the leaf where produced pheromones are accumulated to be released in a burst upon stimuli.

The pheromone molecules are produced at a rate $s(t)$ $(mol\ m^{-2}s^{-1})$ and then they are stored in both aqueous and lipid phase storage pools inside the cells [32]. These storage pools arise from the fact that produced pheromones inside the cells must diffuse to the intercellular air space through the cells of the leaf which consist of aqueous compartments and lipid cell membranes regardless where they are produced [29]. If a pheromone is soluble in the water it is stored in aqueous pools inside the cells whereas if it is soluble in lipids, it is stored in lipid pools inside the cells. Then, the stored pheromone molecules diffuse to the intercellular air space where they are stored in gas pools since they take a gas form. The pheromones in the gas pools in the intercellular air space diffuse through the stomata to the ambient air.

The partitioning ratio between the aqueous and lipid phases are determined by an empirical coefficient, η. These temporary storage pools are designated as S_a for aqueous phase and S_l for lipid phase. k_a denotes the rate of release from the aqueous storage pool (S_a) whereas k_l denotes the rate of release from the lipid storage pool (S_l), both depend on the complex diffusion pathway within the leaf and the physico-chemical characteristics of the pheromone such as its Henrys law and diffusion constants and the physical characteristics of the leaf such as its area and volume. The pheromones then go into the gas phase stored in the gas phase pool S_g in the leaf intercellular air space. The flux of pheromones out of the gas phase pool to the ambient air has a rate k_g which depends on the gas phase conductance from the cell walls to the intercellular air space and the conductance from intercellular air space to the ambient air. Also, the kinetic constants k_a,k_l, and k_g are all related to leaf structural properties defining the size of the pools within the leaf and the conductances between pools and their unit is s^{-1} [32].

The pheromone release process from leaves is described in Fig. 3 where the emission rate to the air is denoted by $q(t)$ [32]. The existence of the described storage pools are experimentally verified and the transition parameters between the pools are identified in the literature [34], [35].

The dynamics of the aqueous, lipid and gas phase pools described in Fig. 3 are modeled by [32] as a system of differential equations as follows

$$\frac{dS_a(t)}{dt} = \eta s(t) - k_a S_a(t), \tag{1}$$

$$\frac{dS_l(t)}{dt} = (1-\eta) s(t) - k_l S_l(t), \tag{2}$$

$$\frac{dS_g(t)}{dt} = k_a S_a(t) + k_l S_l(t) - k_g S_g(t). \tag{3}$$

Then, the emission rate of the volatile from the leaf is

$$q(t) = k_g S_g(t). \tag{4}$$

The signal to be transmitted is denoted by $s(t)$ and the emitted signal by the leaves of the plants is denoted by $q(t)$. Then, the Fourier Transform of the transfer function for the transmitter can be found by

$$H_T(f) = \frac{Q(f)}{S(f)} \tag{5}$$

where $Q(f)$ and $S(f)$ are the Fourier Transforms of the pheromone emission rate into the air and the pheromone production rate, respectively.

Taking the Fourier Transforms of (1-4), the transfer function for the transmission block can be found by

$$H_T(f) = \frac{k_g}{(j2\pi f + k_g)} \left(\frac{k_a \eta}{j2\pi f + k_a} + \frac{k_l(1-\eta)}{j2\pi f + k_l} \right). \quad (6)$$

The partition ratio of the pheromone into the aqueous and lipid pools, η, depends on the solubility and the diffusion coefficient of the pheromone. Since most of the pheromones are water soluble [22], we consider that pheromones occupy only the aqueous pool which results in $\eta = 1$. Then, the transfer function is simplified to

$$H_T(f) = \frac{k_g}{(j2\pi f + k_g)} \frac{k_a}{(j2\pi f + k_a)}. \quad (7)$$

Using the Fourier Transform of the transfer function in (7), we can derive the normalized gain and delay for the transmission process.

The normalized gain $\Gamma_T(f)$ for the transmission process is the magnitude $|H_T(f)|$ of the transfer function $H_T(f)$ normalized by its maximum value $\max_f(|H_T(f)|)$ expressed as

$$\Gamma_T(f) = \frac{|H_T(f)|}{\max_f(|H_T(f)|)} = \frac{k_g k_a}{\sqrt{k_g^2 + (2\pi f)^2}\sqrt{k_a^2 + (2\pi f)^2}}. \quad (8)$$

The delay $\tau_T(f)$ for the transmission process is:

$$\tau_T(f) = -\frac{d\phi_E(f)}{df} = \frac{2\pi}{k_a \left(1 + \left(\frac{2\pi f}{k_a}\right)^2\right)} + \frac{2\pi}{k_g \left(1 + \left(\frac{2\pi f}{k_g}\right)^2\right)} \quad (9)$$

where $\phi_E(f)$ is the phase of the transfer function of

$$\begin{aligned} \phi_E(f) &= \arctan\left(\frac{Im(H_E(f))}{Re(H_E(f))}\right) \\ &= \arctan(-2\pi f/k_g) + \arctan(-2\pi f/k_a) \end{aligned} \quad (10)$$

which is computed from the real part $Re(H_T(f))$ and the imaginary part $Im(H_T(f))$ of the transfer function $H_T(f)$.

For the transmission process, the normalized gain in (8) represents how the pheromone signal is attenuated while diffusing from the cells to the intercellular air space and then to the air. The delay of this process in (9) represents the distortion effect of the time required for this diffusion.

III. The Propagation Process of Pheromone Signals

After the emission of pheromone from plant cells into the environment, the pheromone molecules are transported to the receivers by the help of the flow in the environment which might be the flow of the sea for aquatic plants or the flow of air for plants growing on the soil. In this section, we describe the dispersion of the pheromones in the air under the influence of the wind and turbulent diffusion.

Firstly, we consider the channel when the wind is constant. In the literature [23], [26], [27], meteorological measurements for the wind velocity is collected every 10 min which is also the time step for simulators of turbulent diffusion in the air. Since the maximum distance that we consider is 200 m and the slowest wind speed we consider is 1 m/s, the maximum delay will be $\tau = 200/1 = 200s$ which is smaller than 10 min. Hence, pheromone channel can be modeled as a time invariant channel for 10 min windows. The turbulence due to the atmospheric instability will be incorporated to the channel model with a constant wind solution.

The message to be transmitted is encoded on the rate of the emitted pheromone molecules, i.e., $q(t)$, in the emission process. The emitted pheromone molecules are dispersed through the environment and creates a concentration profile in the direction of wind. The concentration at a position $\vec{x} = (x, y, z) \in R^3$ $[m]$ and at time $t \in R$ $[s]$ is described by a function $c(\vec{x}, t)$ $[kg/m^3]$. Our goal is to find the concentration $c(\vec{x}, t)$ in an arbitrary receiver location in the downwind area in terms of the emission rate $q(t)$.

According to the law of conservation of mass, the time derivative of $c(\vec{x}, t)$ is expressed as

$$\frac{\partial c(\vec{x}, t)}{\partial t} + \nabla \cdot \vec{J}(\vec{x}, t) = S(\vec{x}, t) \quad (11)$$

where $S(\vec{x}, t)$ $[kg/m^3 s]$ represents a source term, and the vector function $J(\vec{x}, t)$ represents the mass flux $[kg/m^2 s]$ of pheromone due to advection and diffusion found by

$$\vec{J} = \vec{J}_A + \vec{J}_D = c\vec{u} - K\nabla c. \quad (12)$$

The first contribution to the flux is the advection by the wind denoted by $\vec{J}_A$, and it is found by $\vec{J}_A = C\vec{u}$ where $\vec{u}$ $[m/s]$ is the wind velocity.

The second contribution to the flux is the atmospheric diffusion arising from the turbulent eddy motion in the atmosphere. According to Fick's law, the diffusive flux changes linearly with the concentration gradient, i.e., $\vec{J}_D = -K\nabla c$. The diffusion coefficient K represents the turbulent eddy diffusivities in (x, y, z) directions in a diagonal matrix. The negative sign in the expression guarantees the flow of molecules from high concentration regions to low concentration regions.

By substituting (12) in (11) we obtain the diffusion-advection equation in three dimensions as

$$\frac{\partial c}{\partial t} + \nabla \cdot (c\vec{u}) - \nabla \cdot (K\nabla c) = S. \quad (13)$$

In order to obtain a closed-form analytical solution, we make a number of simplifying assumptions. Firstly, we consider that the wind velocity is constant and the wind is aligned with the positive x axis, i.e., $\vec{u} = (u, 0, 0)$ for a constant u. Secondly, the diffusion is isotropic and the eddy diffusivities depend only on the downwind distance x, i.e.,

$$K_x(x) = K_y(x) = K_z(x) =: K(x). \quad (14)$$

Thirdly, we assume that the wind velocity is significantly large so that the diffusion in x-direction is negligible, i.e.,

$$K(x)\frac{\partial c}{\partial x} = 0. \quad (15)$$

This assumption is widely accepted by the literature [26], [36]–[39] for turbulent diffusion under the effect of wind.

Finally, we assume that the topography does not change much in the considered area so that the ground is taken as a flat surface at the plane $z = 0$.

To obtain the impulse response of the dispersion process, we consider the emitting plant as an instantaneous and time-varying point source which has a pheromone emission rate $q(\vec{x}, t)$ defined in Section II expressed as

$$q(\vec{x}, t) = Q_T \delta(x)\delta(y)\delta(z - H)\delta(t), \tag{16}$$

where H is the height of the emitting leaf according to the ground, Q_T is the total amount of pheromone released at $t = 0$. Since we are considering a point source 16 contains $\delta(x)\delta(y)\delta(z - H)$ term representing the position of the emission as $(0, 0, H)$.

When we substitute $S(\vec{x}, t)$ in (13) with $q(\vec{x}, t)$ in (16) and take into consideration all the above assumptions, (13) becomes

$$\frac{\partial c}{\partial t} + u\frac{\partial c}{\partial x} - K(x)\frac{\partial^2 c}{\partial y^2} - K(x)\frac{\partial^2 c}{\partial z^2} = Q_T \delta(x)\delta(y)\delta(z - H)\delta(t), \tag{17}$$

where $u\frac{\partial c}{\partial x}$ represents the drag by the wind in x-axis, $K(x)\frac{\partial^2 c}{\partial y^2}$ and $K(x)\frac{\partial^2 c}{\partial z^2}$ represent the turbulent diffusion in y- and z-axes.

Since we are concerned with the concentration of pheromone in the downwind direction, we look for solutions to (17) for $x, z \in [0, \infty)$ and $y \in (-\infty, \infty)$. To solve the partial differential equation (17), we need to specify the boundary conditions such as

$$c(0, y, z, t) = 0, \tag{18a}$$
$$c(\infty, y, z, t) = 0, \tag{18b}$$
$$c(x, \pm\infty, z, t) = 0, \tag{18c}$$
$$c(x, y, \infty, t) = 0, \tag{18d}$$
$$K(x)\frac{\partial c}{\partial z}(x, y, 0, t) = 0. \tag{18e}$$

(18a) represents that we consider only one source of pheromone at $x = 0$, and there is no pheromone concentration for $x < 0$. (18b)-(18d) represents the condition that the total mass of the pheromone should remain finite. Thus, we set the concentration to zero at infinity. (18e) is the final boundary condition where $K(x)$ is defined in (14) which reflects that there is no vertical flux at ground, i.e., pheromones do not penetrate the ground.

Now, we have a well-defined problem for the dispersion of pheromones in the air with the partial differential equation in (17) and the boundary conditions in (18).

Using Stakgold's theorem in [18], we reformulate the problem in (17) as

$$\frac{\partial c}{\partial t} + u\frac{\partial c}{\partial x} - K(x)\frac{\partial^2 c}{\partial y^2} - K(x)\frac{\partial^2 c}{\partial z^2} = 0, \tag{19}$$

and we modify the boundary condition in (18a) as

$$c(0, y, z) = \frac{Q_T}{u}\delta(y)\delta(z - H)\delta(t). \tag{20}$$

The eddy diffusivities $K(x)$ in (19) are hard to determine in practice since they vary with weather conditions and downwind distance. Thus, we define a new variable r with units of $[m^2]$ such as

$$r = \frac{1}{u}\int_0^x K(\xi)d\xi. \tag{21}$$

By applying this change of variables, the eddy diffusivities K are eliminated from (19) and we obtain a new problem for $c'(r(x), y, z, t) := c(x, y, z, t)$ expressed as

$$\frac{\partial c'}{\partial t} + \frac{\partial c'}{\partial r} = \frac{\partial^2 c'}{\partial y^2} + \frac{\partial^2 c'}{\partial z^2}, \tag{22}$$

for which the boundary conditions are the same as in (18) with x replaced with r.

Then, the separation of variables method is applied to (22) such that $c'(r, y, z, t)$ can be expressed as

$$c'(r, y, z, t) = \frac{Q_T}{u}a(r, y)b(r, z)p(r, t). \tag{23}$$

Hence, we obtain three reduced dimensional problems for each of the functions $a(r, y)$, $b(r, z)$, and $p(r, t)$. The partial differential equation with boundary conditions for $a(r, y)$ is

$$\frac{\partial a(r, y)}{\partial r} = \frac{\partial^2 a(r, y)}{\partial y^2}, \text{ for } 0 \le r < \infty \text{ and } -\infty < y < \infty \tag{24a}$$

$$a(0, y) = \delta(y),\ a(\infty, y) = 0,\ a(r, \pm\infty) = 0, \tag{24b}$$

and the partial differential equation with boundary conditions for $b(r, z)$ is

$$\frac{\partial b(r, z)}{\partial r} = \frac{\partial^2 b(r, z)}{\partial z^2}, \text{ for } 0 \le r < \infty \text{ and } 0 < z < \infty \tag{25a}$$

$$b(0, z) = \delta(z - H),\ b(\infty, z) = 0,\ b(r, \infty) = 0,\ \frac{\partial b}{\partial z}(r, 0) = 0, \tag{25b}$$

which both have the form of 2D diffusion equations. The partial differential equation with boundary conditions for $p(r, t)$ is

$$\frac{\partial p(r, t)}{\partial t} = -\frac{\partial p(r, t)}{\partial r}, \text{ for } 0 \le r < \infty \text{ and } 0 < t < \infty \tag{26a}$$

$$p(0, t) = \delta(t),\ p(\infty, t) = 0,\ p(r, \infty) = 0, \frac{\partial p}{\partial t}(r, 0) = 0. \tag{26b}$$

There are more than one method to solve the problems (24), (25), (26) using approaches based on infinite series and Fourier transform techniques [19], similarity methods [20], Green's functions [21] or Laplace transforms [23].

In this paper, we use Laplace transformation to obtain the solution for the reduced problems (24), (25), and (26) since this approach can be extended to solve more complicated problems such as pheromone dispersion with deposition on the ground or with anisotropic eddy diffusivities.

To begin with, we first consider the Laplace transform of $a(r, y)$ in r where the Laplace transform in r is defined as $\hat{a}(\rho, y) := \mathscr{L}\{a(r, y)\} = \int_0^\infty e^{-\rho r}a(r, y)dr$ and ρ is the transform variable. Then, (24) becomes

$$\rho\hat{a} - a(0, y) = \frac{\partial^2 \hat{a}}{\partial y^2}. \tag{27}$$

Applying the boundary condition for source in (24b), we obtain

$$\frac{\partial^2 \hat{a}}{\partial y^2} - \rho \hat{a} = -\delta(y). \tag{28}$$

Then, we take the Laplace transform of $\hat{a}(\rho, y)$, i.e., $\hat{\hat{a}}(\rho, \mu) := \mathscr{L}\{\hat{a}(\rho, y)\} = \int_0^\infty e^{-\mu y} \hat{a}(\rho, y) dy$ with the transform variable μ. Then, (28) becomes

$$\mu^2 \hat{\hat{a}} - \mu \hat{a}(\rho, 0) - \frac{\partial \hat{a}}{\partial y}(\rho, 0) - \rho \hat{\hat{a}} = -1. \tag{29}$$

By factorizing (29), we obtain

$$\hat{\hat{a}}(\rho, \mu) = \frac{\eta \hat{a}(\rho, 0) + (\frac{\partial \hat{a}(\rho,0)}{\partial_y} - 1)}{\mu^2 - \rho}. \tag{30}$$

By applying inverse Laplace transform in μ to (30), we obtain

$$\hat{a}(\rho, y) = \frac{\partial \hat{a}(\rho, 0) - 1}{\sqrt{\rho}} e^{-\sqrt{\rho} y}. \tag{31}$$

Assuming that $\partial \hat{a}(\rho, 0)$ is independent of ρ, we now apply inverse Laplace transform in ρ to (31) and get

$$a(r, y) = \frac{1}{\sqrt{4\pi r}} e^{-y^2/4r}, \tag{32}$$

where the delta function identity, i.e., $\delta(y) = \lim_{r \to 0} exp(-y^2/4r)/\sqrt{4\pi r}$, is used.

By following similar procedures for the systems described in (25) and (26), we can find $b(r, z)$ such as

$$b(r, z) = \frac{1}{\sqrt{4\pi r}} \left(e^{-(z-H)^2/4r} + e^{-(z+H)^2/4r} \right) \tag{33}$$

and $p(r, t)$ such as

$$p(r, t) = \frac{u}{\sqrt{4\pi r}} e^{-(x-ut)^2/4r}. \tag{34}$$

Substituting (32), (33), and (34) in (23), and using the definition $c'(r, y, z, t) = c(\vec{x}, t)$, the solution for the pheromone concentration is found as

$$c(\vec{x}, t) = \frac{Q_T}{8(\pi r)^{3/2}} e^{(-(x-ut)^2 - y^2)/4r} \left[e^{-(z-H)^2/4r} + e^{-(z+H)^2/4r} \right], \tag{35}$$

The expression in (35) represents a concentration profile of pheromones emitted instantaneously from the transmitter plant in 3-D. This profile has the shape of a puff dragged in the wind direction and expanding in the other directions. Since the concentration follows a Gaussian distribution, the pheromone concentration profile is called *Gaussian puff* which is illustrated in Fig. 4.

In the case of anisotropic eddy diffusivities for y and z directions, i.e., $K_y(x) \neq K_z(x)$, the concentration profile in (35) can be derived as

$$c(\vec{x}, t) = \frac{Q_T}{8(\pi \sqrt{r_y r_z})^{3/2}} e^{\frac{(-(x-ut)^2)}{4\sqrt{r_y r_z}}} e^{\frac{(-y^2)}{4r_y}} \left[e^{\frac{-(z-H)^2}{4r_z}} + e^{\frac{-(z+H)^2}{4r_z}} \right], \tag{36}$$

following a similar derivation where r is redefined as $r_{y,z}(x) = \frac{1}{u} \int_0^x K_{y,z}(\xi) d\xi$.

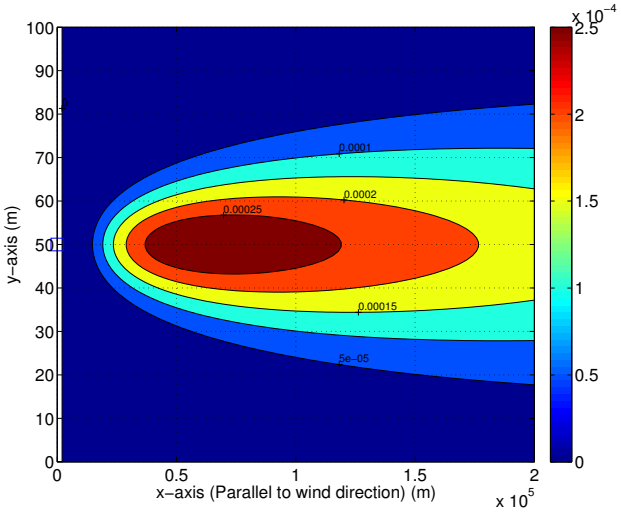

Fig. 4. The concentration profile of the emitted pheromone molecules from the transmitter at $(x, y) = (0.2, 50)$ which is a Gaussian puff. It is observed that the puff is in the x-direction parallel to wind.

Up to now, we considered constant eddy diffusivities. However, due to effect of turbulence, eddy diffusivities change with the downwind distance. The relation between the diffusivities and the downwind distance are is very difficult to determine theoretically, therefore empirical studies are conducted for various atmospheric conditions. As a result, Pasquill atmospheric stability classes are defined according to the wind speed and the standard deviations of the horizontal and vertical fluctuations [24]. There are 6 stability classes from A to F, where A is the very unstable class and F is the stable class. For the rest of this study, we consider the stable class F where the standard deviation of the angle of wind is below $3.4°$. Then, the eddy diffusivities can be expressed as

$$\begin{aligned} r_y(x) &= \frac{0.08x^2}{1 + 0.0001x} \\ r_z(x) &= \frac{0.000128x^2}{(1 + 0.0003x)^2}, \end{aligned} \tag{37}$$

for rural areas [25].

Since we consider an impulse in time as input expressed in (16), taking the Fourier Transform of (35) directly gives us the transfer function of the dispersion process $H_P(f)$ found by

$$H_P(f) = C(\vec{x}, f) = \mathcal{F}\{c(\vec{x}, t)\}. \tag{38}$$

Thus, the transfer function $H_P(f)$ is expressed as

$$H_P(f) = H_0 e^{-\frac{4\pi^2 \sqrt{r_y r_z}}{u^2} f^2} e^{-j \frac{x}{u} 2\pi f} \tag{39}$$

where

$$H_0 = \frac{1}{4\pi \sqrt{r_y r_z} u} e^{-y^2/4r_y} \left[e^{-(z-H)^2/4r_z} + e^{-(z+H)^2/4r_z} \right]. \tag{40}$$

The normalized gain $\Gamma_P(f)$ for the dispersion process is expressed by

$$\Gamma_P(f) = \frac{|H_P(f)|}{\max_f(|H_P(f)|)} = e^{-\frac{4\pi^2 \sqrt{r_y r_z}}{u^2} f^2}. \tag{41}$$

This article has been accepted for publication in a future issue of this journal, but has not been fully edited. Content may change prior to final publication. Citation information: DOI 10.1109/TNB.2016.2628047, IEEE Transactions on NanoBioscience

The delay $\tau_P(f)$ for the dispersion process is:

$$\tau_P(f) = -\frac{d\phi_P(f)}{df} = 2\pi\frac{x}{u} \tag{42}$$

where $\phi_P(f)$ is the phase of the transfer function $H_P(f)$ found by

$$\phi_P(f) = \arctan\left(\frac{Im(H_P(f))}{Re(H_P(f))}\right). \tag{43}$$

Note that, the delay τ_P is proportional to x/u, which is the time required for wind to arrive to a location x away from the source with velocity u. Moreover, since we ignored the diffusion on the wind direction, the phase for the dispersion process is linear.

IV. The Reception Process of Pheromone Signals

The pheromone molecules arriving to the destination plant are captured by the leaves of the plant. The gas exchange through stomata on the leaves enables the intake of pheromones into the leaves as shown in Fig. 5 [40].

The diffusive net flux between the atmosphere and the leaves for this gas exchange is expressed as

$$\Phi = Ag[c(\vec{x},t) - C_L(t)/K_{LA}], \tag{44}$$

where A is the leaf surface area, g is the conductance, K_{LA} is the partition coefficient between air and leaves which is the concentration ratio between two neighboring phases in thermodynamic equilibrium, $c(\vec{x},t)$ is the gas phase concentration in the air and $C_L(t)$ is the concentration in the leaves [40]. The first term on the right hand side represents the diffusion into the leaf of incoming pheromone concentration and the second term represents the diffusion of the pheromone concentration from the leaves back into the air.

If we consider the mass balance for the leaf, the change of chemicals in aerial part of the leaf is expressed as

$$\frac{dm(t)}{dt} = \Phi, \tag{45}$$

where $m(t)$ is the mass of chemicals in aerial part of the leaf [40]. Then by dividing (45) by the volume of the leaf V_L we can express the change of concentration inside the leaves by

$$\frac{dC_L(t)}{dt} = -\left(\frac{Ag}{K_{LA}V_L}\right)C_L(t) + \left(\frac{Ag}{V_L}\right)c(\vec{x},t), \tag{46}$$

where V_L is the volume of the leaves [40].

Then, by taking the Fourier transform of (46), we can obtain the transfer function for the reception process, $H_R(f)$, which is expressed as

$$H_R(f) = \frac{\mathcal{F}\{C_L(t)\}}{\mathcal{F}\{c(\vec{x},t)\}} = \frac{\beta}{j2\pi f + \alpha}, \tag{47}$$

where $\alpha = Ag/(K_{LA}V_L)$ and $\beta = g(A/V_L)$.

The normalized gain for the reception process, $\Gamma_R(f)$, is derived from (47) as

$$\Gamma_R(f) = \frac{|H_R(f)|}{\max_f(|H_R(f)|)} = \frac{\alpha}{\sqrt{\alpha^2 + 4\pi^2 f^2}}. \tag{48}$$

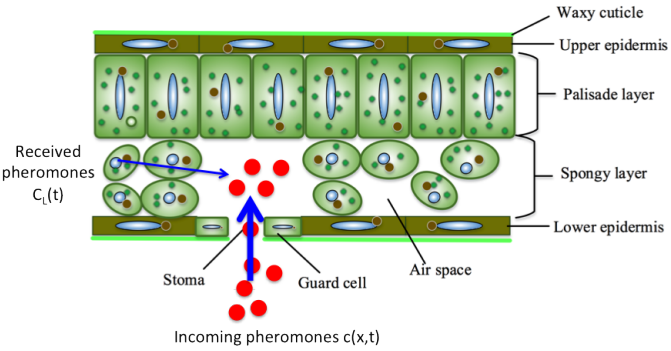

Fig. 5. Reception of pheromone molecules.

The delay for the reception process, $\tau_R(f)$, is derived from (47) as

$$\tau_R(f) = -\frac{d\phi_R(f)}{df} = \frac{2\pi}{\alpha\left(1 + \left(\frac{2\pi f}{\alpha}\right)^2\right)} \tag{49}$$

where $\phi_R(f)$ is the phase of the transfer function $H_R(f)$ which is found by

$$\phi_R(f) = \arctan\left(\frac{Im(H_R(f))}{Re(H_R(f))}\right) = -\arctan\left(\frac{2\pi f}{\alpha}\right). \tag{50}$$

The normalized gain in (48) represents how the pheromone signal is attenuated while diffusing from the air into the leaf through stomata. The delay of this process in (49) represents the time required for this diffusion.

The absorbed pheromones by the plants enable multiple biochemical reactions inside the leaf. After the absorption into stomatal cavities, pheromones diffuse inside the plant cell where they are degraded to several chemicals triggering physiological reactions such as herbivore repellent production and cell growth. These processes are not fully characterized and left for future studies.

V. Numerical Results

In order to fully understand the behavior of the pheromone communication, it is needed to build an end-to-end model including all three basic steps of communication, namely, transmission, propagation and reception.

The metrics characterizing our pheromone channel are the normalized gain and delay derived from the transfer function of the whole system which can be found by

$$H(f) = H_T(f) \cdot H_P(f) \cdot H_R(f), \tag{51}$$

where $H(f)$ is the frequency response of the total system, $H_T(f)$, $H_P(f)$, $H_R(f)$ are obtained from (8), ((39)), (47), respectively.

Hence the normalized gain of the system can be found by

$$\Gamma(f) = \Gamma_T(f) \cdot \Gamma_P(f) \cdot \Gamma_R(f), \tag{52}$$

where $\Gamma(f)$ denotes the normalized gain for the end-to-end system whereas $\Gamma_T(f)$, $\Gamma_P(f)$, $\Gamma_R(f)$ are obtained from (8), (41), and (48), respectively.

This article has been accepted for publication in a future issue of this journal, but has not been fully edited. Content may change prior to final publication. Citation information: DOI 10.1109/TNB.2016.2628047, IEEE Transactions on NanoBioscience

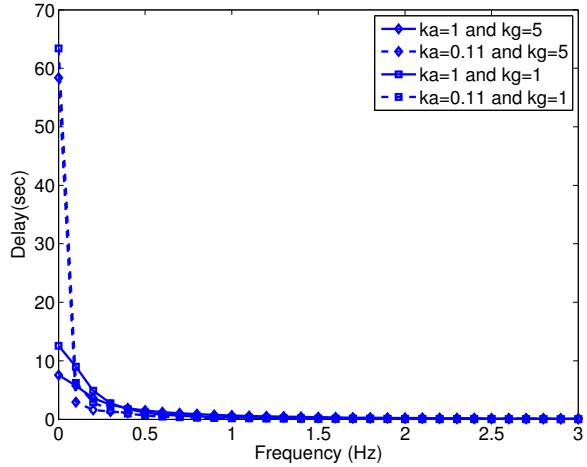

Fig. 6. Delay of the transmission process over frequency.

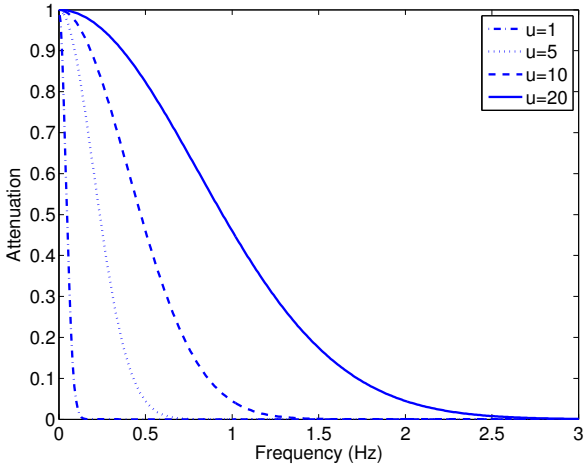

Fig. 8. Attenuation of the propagation process over frequency for various wind speeds.

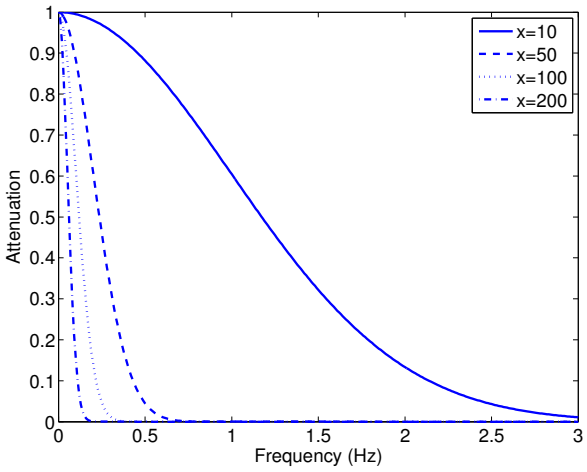

Fig. 7. Attenuation of the propagation process over frequency for various transmitter-receiver distances.

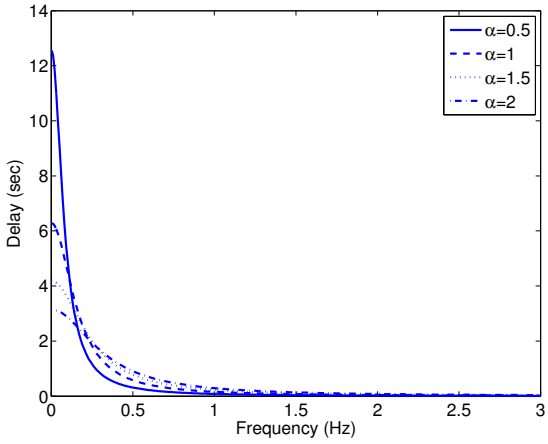

Fig. 9. Delay of the reception process over frequency.

The other metric, the end-to-end delay is found by

$$\tau(f) = \tau_T(f) + \tau_P(f) + \tau_R(f), \tag{53}$$

where τ denotes the group delay for the end-to-end system whereas τ_T, τ_P, τ_R are obtained from (9), (42), and (49), respectively.

In this section, we provide the numerical results for the end-to-end model of the pheromone communication channel. The frequency is swiped between 0-3 Hz which is consistent with the the slow dynamics of plant metabolism [31] and observed pheromone communication dynamics [32] for the considered communication range which is in the order of meters. Even though the bandwidth is very small, it can be extended by changing the properties of the transmitter plant or choosing different pheromone molecules with higher volatility.

Firstly we consider the delay of the transmission process illustrated in Fig. 6. The delay for $k_g = 0.11, 5\ s^{-1}$ and $k_a = 1, 5\ s^{-1}$ dynamic constants for linalool emitted from different leaf types are plotted [33]. It is observed that the maximum delay is around 65 sec and it decreases sharply with the frequency. It can be concluded that for high frequencies the delay of the transmission process is not significant. This arises from the fact that the chosen pheromone is diffusing quickly inside the leaf cells.

Now, we look for the effects of propagation process. In Fig.

This article has been accepted for publication in a future issue of this journal, but has not been fully edited. Content may change prior to final publication. Citation information: DOI 10.1109/TNB.2016.2628047, IEEE Transactions on NanoBioscience

7, only the effect of the propagation process on the attenuation is shown for different transmitter-receiver distances using (41). For a wind velocity $u = 5$ m/s, it is observed that the signal is more attenuated with increasing distance which is expected. As the pheromone puff is moving from the transmitter plant to the receiver plant on x-axis under the drift of the air, it diffuses more in y and z axes with the increasing distance. Hence, the concentration drops shown as the increased attenuation.

Another factor affecting the propagation process is the velocity of the wind. In this study, we considered a constant wind condition where the speed and the direction of the wind does not change significantly with time. In Fig. 8, attenuation for a transmitter-receiver distance of 100 m is shown for different wind speeds using (41). As shown in Fig. 8, a faster wind can carry signals of higher frequency since pheromone molecules do not have enough time to diffuse in x direction causing the widening of the pulse which limits the bandwidth. Usually, in a small geographical area, the prevailing wind is determined with an average speed and an average direction which vary. The stochastic channel model is left for future study.

We omitted the plot for the delay of the propagation process since the delay does not change with the frequency according to 42. This phenomenon arises from the fact that the diffusion in x-axis is neglected, the delay is just the time required for the signal to travel from the transmitter to the receiver with the drift of the wind.

Furthermore, we plotted the delay of the reception process in Fig. 9. The delay is plotted for $\alpha = 0.5, 1, 1.5, 2$ corresponding to different leaf types and sizes. The delay is observed to be bounded to 13 sec for increasing frequency. Fig. 6 and Fig. 9 show us that the limiting delay for the proposed communication system are not caused by the transmission and reception processes.

Now, by considering all three steps of pheromone channel altogether, we evaluated the attenuation and delay of the channel using (52) and (53), respectively. The wind speed is $u = 5$ m/s [32]. The parameters for the emission from the leaf are $k_g = 1\ s^{-1}$ and $k_a = 5\ s^{-1}$ [32], and the parameters for reception by the leaf are $\alpha = 0.9\ s^{-1}$. Fig. 10 shows the attenuation of the end-to-end model. It is observed that the attenuation increases with distances. Also, transmission and reception processes lowers the bandwidth since attenuation is more severe compared to Fig. 7 which shows only the attenuation due to the propagation process.

The delay characteristics of the end-to-end model for the pheromone channel is shown in Fig. 11 for different transmitter-receiver distances. It is observed that as the distance increases the delay increases since it takes more time for the pheromone molecules to be carried to the destination. Also, it is observed that the end-to-end-delay is dominated by the delay of propagation. The delay converges to the time required for the wind to reach the destination which is the ratio of the transmitter-receiver distance to wind speed since in this region the drift of the molecules becomes dominant over the diffusion.

Considering the numerical evaluations, it is possible to say that the pheromone communication channel has a limited

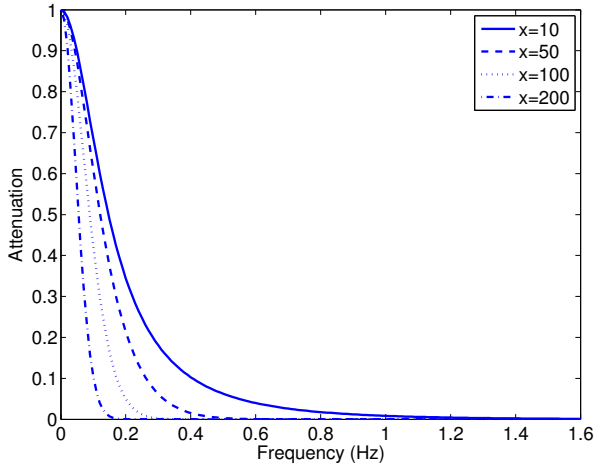

Fig. 10. Attenuation of the end-to-end channel.

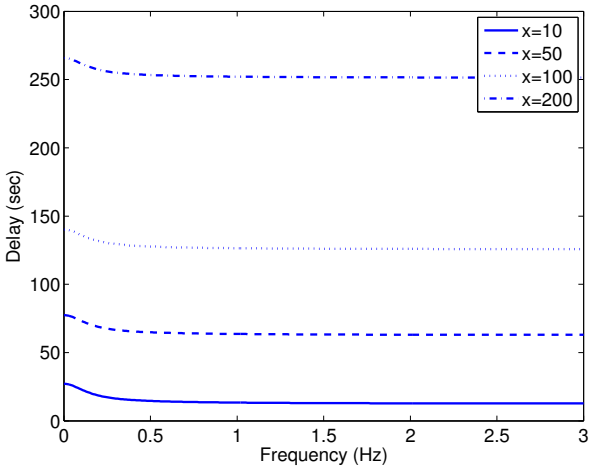

Fig. 11. Delay of the end-to-end channel.

bandwidth of approximately a few Hz. Hence, the capacity will not be very high compared to electromagnetic communication. However, the information processing in biology usually takes hours to be completed. Thus, the bandwidth of the pheromone channel is enough to cope with the biological applications of molecular communication.

VI. Conclusion

Although molecular communication is a nanoscale paradigm, there are applications requiring macroscale tasks. Due to its long range up to few hundred meters as demonstrated in the paper, pheromone communication channel constitutes a solution for extending the range of molecular communication to macroscale. Furthermore, the natural abundance and the diversity of pheromones carrying messages in between the same species and among different species provide us with many examples for building artificial devices which exploit pheromone communication.

In this paper, the characteristics of pheromone channels are investigated in terms of attenuation and delay for pheromone communication in plants. The pheromone communication consists of transmission, propagation and reception processes. In transmission process, the pheromone molecules are emitted from the leaves of the plants in to the air where they are propagated by the flow of the air. In dispersion process, the pheromone molecules are dragged in the direction of wind which carries the pheromone molecules to the receiver plant. In the reception process, pheromone molecules are captured by the leaves of the receiver plant and decoded according to the received concentration.

ACKNOWLEDGMENT

The authors would like to thank Massimiliano Pierobon, Youssef Chahibi, A. Ozan Bicen for their excellent and constructive feedback which helped to improve the quality of the paper.

REFERENCES

[1] M. Pierobon, and I. F. Akyildiz, "Capacity of a diffusion-based molecular communication system with channel memory and molecular noise," *IEEE Transactions on Information Theory,* vol. 59, no. 2, pp. 942954, Feb. 2013.

[2] A. O. Bicen, and I. F. Akyildiz, "System-theoretic analysis and least-squares design of microfluidic channels for flow-induced molecular communication," *IEEE Transactions on Signal Processing,* vol. 61, no. 20, pp. 5000-5013, Oct. 2013.

[3] M. Gregori, and I. F. Akyildiz, "A new nanonetwork architecture using flagellated bacteria and catalytic nanomotors," *IEEE Journal on Selected Areas in Communications,* vol. 28, no. 4, pp. 612-619, May 2010.

[4] M. Moore, A. Enomoto, T. Nakano, R. Egashira, T. Suda, A. Kayasuga, H. Kojima, H. Sakakibara, and K. Oiwa, "A design of a molecular communication system for nanomachines using molecular motors, in *Proc. of Fourth Annual IEEE International Conference on Pervasive Computing and Communications Workshops,* March 2006, pp. 612.

[5] T. D. Wyatt, "Pheromones and animal behaviour: communication by smell and taste," *Cambridge University Press,* 2003.

[6] W. H. Bossert, and E. O. Wilson, "The analysis of olfactory communication among animals," *Journal of theoretical biology,* vol. 5, no. 3, pp. 443-469, 1963.

[7] I. T. Baldwin, et al., "Volatile signaling in plant-plant interactions:" talking trees" in the genomics era." *Science,* vol. 311, no. 5762, pp. 812-815, 2006.

[8] T. Strand, et al., "A simple model for simulation of insect pheromone dispersion within forest canopies," *Ecological Modelling,* vol. 220, no. 5, pp. 640-656, 2009.

[9] Y. Fares, P. J. H. Sharpe, and C. E. Magnuson, "Pheromone dispersion in forests." *Journal of Theoretical Biology,* vol. 84, pp. 335-359, 1980.

[10] J. Murlis, J. S. Elkinton, and R. T. Carde, "Odor plumes and how insects use them." *Annual Review of Entomology,* vol. 37, pp. 505-532, 1992.

[11] J. S. Elkinton, R. T. Card, and C. J. Mason, "Evaluation of time-average dispersion models for estimating pheromone concentration in a deciduous forest," *Journal of chemical ecology,* vol. 10, no. 7, pp. 1081-1108, 1984.

[12] M. Pierobon, and I. F. Akyildiz, "A Physical End-to-End Model for Molecular Communication in Nanonetworks," *IEEE JSAC (Journal of Selected Areas in Communications),* vol. 28, no. 4, pp. 602-611, 2010.

[13] T. Nakano, Y. Okaie, and J.-Q. Liu. "Channel model and capacity analysis of molecular communication with Brownian motion." *IEEE Communications Letters,* vol. 16, no.6, pp. 797-800. 2012.

[14] I. F. Akyildiz, B. Fernando, and C. Blazquez, "Nanonetworks: A new communication paradigm," *Computer Networks*, vol. 52, no. 12, pp. 2260-2279, Aug. 2008.

[15] L. P. Gine, and I. F. Akyildiz, "Molecular communication options for long range nanonetworks," *Computer Networks,* vol. 53, no. 16, pp. 2753-2766, 2009.

[16] B. S. Beckett, *Biology: a modern introduction,* Oxford University Press, 1986.

[17] D. L. Wood, R. M. Silverstein, and M. Nakajima, Control of insect behavior by natural products, *Elsevier,* 2013.

[18] I. Stakgold, *Boundary Value Problems of Mathematical Physics, volume II,* The MacMillan Company, New York, pp. 56, 1968.

[19] R. Haberman, *Applied Partial Differential Equations with Fourier Series and Boundary Value Problems,* Pearson Prentice Hall, Upper Saddle River, NJ, 2004.

[20] R. M. M. Mattheij, S. Rienstra, and J. ten Thije Boonkkamp, "Partial Differential Equations: Modeling, Analysis, Computation," *SIAM,* Philadelphia, PA, 2005.

[21] H. S. Carslaw and J. C. Jaeger, *Conduction of Heat in Solids,* Clarendon Press, Oxford, 1959.

[22] J. Zhang, and David M. Webb. "Evolutionary deterioration of the vomeronasal pheromone transduction pathway in catarrhine primates," *Proceedings of the National Academy of Sciences,* vol. 100, no. 14, pp. 8337-8341, 2003.

[23] J. M. Stockie, "The mathematics of atmospheric dispersion modeling," *Siam Review,* vol. 53, no. 2, pp. 349-372, 2011.

[24] F. Pasquill, "The estimation of the dispersion of windborne material," *Meteorology Magasine,* vol. 90, no. 1063, pp. 33-49, 1961.

[25] G. A. Briggs, "Analytical parameterizations of diffusion: The convective boundary layer," *Journal of climate and applied meteorology,* vol. 24, no. 11, pp. 1167-1186, 1985.

[26] Turner, D. Bruce. *Workbook of atmospheric dispersion estimates: an introduction to dispersion modeling.* CRC press, 1994.

[27] T. Mikkelsen, et al. "MET-RODOS: a comprehensive atmospheric dispersion module." *Radiation Protection Dosimetry,* vol. 73, no. 1-4, pp. 45-55, 1997.

[28] G. J. Wagner, "Secreting glandular trichomes: more than just hairs," *Plant Physiology,* vol. 96, no. 3, pp. 675-679, 1991.

[29] R. Grote, R. K. Monson, and . Niinemets, "Leaf-level models of constitutive and stress-driven volatile organic compound emissions," *Biology, controls and models of tree volatile organic compound emissions,* pp. 315-355, Springer Netherlands, 2013.

[30] A. Fahn, *Secretory tissues in plants,* Academic Press., 1979.

[31] A. J. Farrell, et al., "Filament-based atmospheric dispersion model to achieve short time-scale structure of odor plumes," *Environmental fluid mechanics,* vol. 2, no. 1-2, pp. 143-169, 2002.

[32] C. P. Harley, "The roles of stomatal conductance and compound volatility in controlling the emission of volatile organic compounds from leaves," *Biology, controls and models of tree volatile organic compound emissions,* Springer Netherlands, pp. 181-208, 2013.

[33] U. Niinemets, and M. Reichstein. "A model analysis of the effects of nonspecific monoterpenoid storage in leaf tissues on emission kinetics and composition in Mediterranean sclerophyllous Quercus species," *Global Biogeochemical Cycles,* vol. 16, no. 4, pp. 57-1, 2002.

[34] Harley, P., et al. "Environmental controls over methanol emission from leaves." Biogeosciences Discussions 4.4 (2007): 2593-2640.

[35] M. S. Noe, et al. "Emissions of monoterpenes linalool and ocimene respond differently to environmental changes due to differences in physicochemical characteristics," *Atmospheric Environment,* vol. 40, no. 25 pp. 4649-4662, 2006.

[36] S. S. Marsden, J. E. Antman et al. "Interdisciplinary Applied Mathematics," 1993.

[37] S. R. Hanna, G. A. Briggs, and R. P. Hosker, "Handbook on Atmopheric Diffusion," *U.S. Department of Energy, Technical Information Center,* DOE/TIC-11223, 1982.

[38] F. Pasquill, "Atmospheric diffusion," 1968.

[39] M. Roberts, M. J. Reiss, and G. Monger, Advanced biology. Nelson Thornes, 2000.

[40] S. Trapp, and M. Matthies, "Generic one-compartment model for uptake of organic chemicals by foliar vegetation," *Environmental science & technology,* vol. 29, no. 9, pp. 2333-2338, 1995.